THE JOURNAL OF PHYSICAL CHEMISTRY B

Article

pubs.acs.org/JPCB

Experimental and Theoretical Study of the High-Temperature UV−Visible Spectra of Aqueous Hydroquinone and 1,4-Benzoquinone

Fereshteh Samiee,[†,§] Federico N. Pedron,[‡,§] Dario A. Estrin,[*,‡] and Liliana Trevani[*,†]

[†]Faculty of Science, University of Ontario Institute of Technology, 2000 Simcoe Street North, Oshawa L1H 7K4, Ontario, Canada

[‡]Departamento de Química Inorgánica, Analítica y Química Física, and INQUIMAE-CONICET, Facultad de Ciencias Exactas y Naturales, Universidad de Buenos Aires, Ciudad Universitaria, Pab. 2, C1428EHA CABA, Argentina

ABSTRACT: UV−visible spectroscopic studies of aqueous hydroquinone (HQ) and 1,4-benzoquinone (BQ) have been carried out along with classical molecular dynamics (MD) and quantum calculations. The experimental results confirmed that HQ is stable in hot compressed water up to at least 523 K at 70 bar, but BQ decomposes at temperatures lower than 373 K, leading to the formation of HQ and other nonabsorbing products. Even though benzoquinone is not stable, our study significantly extended the temperature range of other spectroscopic studies, and the spectra of HQ up to 523 K can still be useful for other studies, particularly those related to organic species in deep ocean hydrothermal vents. Classical MD simulations at high temperatures show, as expected, a weakening of the solute−solvent H-bonding interactions. The dependence of the maximum absorption of BQ on temperature was also analyzed, although a significant degree of decomposition was observed in the time frame of our experiments. The shift of the maximum absorption peak of BQ with temperature was consistent with time-dependent density functional theory calculations.

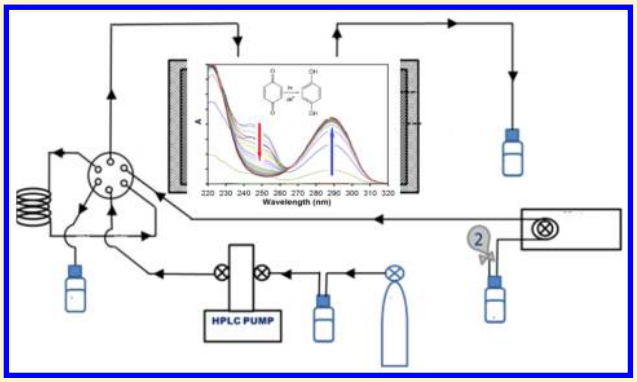

1. INTRODUCTION

The oxidation of HQ to BQ is one of the few electrochemical reactions that has been studied at temperatures over the critical point of water (647.15 K and 220.6 bar). This study showed that HQ has a good chemical stability under hydrothermal conditions in acid media up to 658 K at 270 bar, as long as no O_2 is present in the solution.[1]

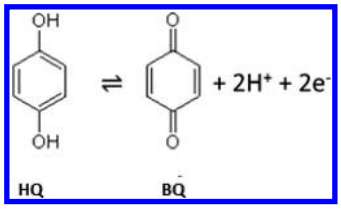

On the other hand, other studies have shown that BQ, the oxidation product of HQ, readily decomposes in the presence of water at relatively low temperatures.[2,3] For instance, Razimov et al.[3] found that BQ polymerizes in water at temperatures as low as 323 K, with the formation of HQ. Because BQ is stable in organic solvents below 493 K and does not undergo thermal bulk polymerization, the authors concluded that the process requires the presence of H_2O or hydroxyl ions to initiate the polymerization reaction.

Xu et al.[2] investigated the role of water in the mechanism of decomposition of BQ under hydrothermal conditions, including supercritical water (SCW). On the basis of the absence of 2-hydroxyl-*p*-benzoquinone and 2,5-dihydroxyl-*p*-benzoquinone in the reaction mixture that could be formed by the reaction of BQ with HO• radicals from water, the authors concluded that the BQ polymerization reaction must follow a reaction pathway similar to the one proposed by Razimov and co-workers.[3] In this model, the activation of quinone molecules takes place via complexation with water molecules or with hydroxyl ions in alkaline solutions; the complex is more nucleophilic than the molecule of quinone, and this explains the electron transfer upon heating. Free H• radicals, formed as a result of the polymerization process, can reduce BQ to HQ or result in the formation of molecular hydrogen, which can also result in the formation of HQ.

Despite the numerous studies on the BQ/HQ system under room temperature conditions due to the role of quinone in biological systems,[4] as biosensors for monitoring biochemical reactions,[5] and, more recently, their potential application in the field of batteries[6,7] and flow batteries,[8] to the best of our knowledge, there is no reported spectroscopic data on HQ or BQ at temperatures above the boiling point of water.

The UV/visible spectrum of HQ showed only small changes on going from room temperature to 523 K, but because BQ readily decomposes in water at low temperature, a significant reduction in absorbance is observed in the spectrum of this

Received: August 4, 2016
Revised: September 9, 2016
Published: September 14, 2016

DOI: 10.1021/acs.jpcb.6b07893
J. Phys. Chem. B 2016, 120, 10547−10552

species between room temperature and 373 K. Nevertheless, the main absorption bands for BQ could be determined from the differential and normalized spectra.

Tossell[9] has performed detailed energetic, geometric, and spectroscopic quantum mechanical (QM) calculations for HQ, BQ, and their complexes at room temperature, with the goal of understanding their roles as model components in humic acids. In this study, we have performed classical molecular dynamics (MD) simulations using the Amber MD Package[10] to study the solvations of both HQ and BQ at 300 K at 1 bar and 300, 373, 423, 473, and 523 K at 70 bar. In addition, linear response time-dependent density functional theory (TD-DFT) calculations were carried out with the polarizable continuum model (PCM)[11] for describing solvent effects, using Gaussian 09 software.[12] Both the static dielectric constant and optical dielectric constant were adjusted to the proper values at the corresponding temperatures and pressures.

2. EXPERIMENTAL AND THEORETICAL METHODS

All chemicals were purchased from Sigma-Aldrich at the highest available grade and used without further purification: 1,4-benzoquinone (BQ, ≥98%; Sigma-Aldrich), hydroquinone (HQ, ≥99%; Sigma-Aldrich), and sodium bisulfate monohydrate ($NaHSO_4 \cdot H_2O$, 99%; Sigma-Aldrich). Solutions were prepared by mass using oxygen-free deionized water, with a resistivity of 18 MΩ cm, that was prepared by bubbling argon gas (GP-S20078A; Praxair) in an air-tight bottle overnight. The concentrations of benzoquinone and HQ in the solutions were kept within 10^{-4} and 10^{-5} m to avoid extremely high absorbance values, and $NaHSO_4$ was used to adjust the pH of the solutions.

2.1. High *T*, *p* Spectroscopic Cell and Injection System. The UV−visible system used to carry out the spectroscopic measurements is similar in design to the one used by Trevani et al.[13] for studying copper ammonia complexation reactions under hydrothermal conditions. Briefly, the injection system is composed of a high-pressure (ISCO D-Series) pump (1) that is used to circulate water through the system at a constant flow rate (1 cm^3/min) under high-pressure conditions, a titanium six-port valve (2) that allows injection of the solution into the titanium preheater and cell (3), a high T, p UV−visible cell with sapphire windows and an optical path length, b, equal to 2.3 cm (4), two on−off valves that can be used to isolate the cell for studies without flow (5), and a cooler and back-pressure regulator (7) at the end of the line to keep the solution (or water) under high-pressure conditions (Figure 1). The cell and preheater were heated using an OMEGA temperature controller (model CSC32) with a thermocouple to control and measure the temperature of the cell. The pressure was set at 70 bar to ensure that the solvent was in the liquid phase over the entire temperature range. Because the polyetheretherketone (PEEK) loop (80 cm^3) used to inject the solution into the cell is relatively large, a low-pressure peristaltic pump (Masterflex L/S economy drive) was used to fill the sample loop from an oxygen-free bottle containing the HQ or BQ solutions. Only PEEK, poly(tetrafluoroethylene), and titanium were in contact with the solutions. A Cary 50 spectrophotometer (190−1100 nm) was used to record the absorption spectra at temperatures between 298 and 523 K. All spectra were recorded at 1 nm wavelength intervals from 200 to 800 nm, at a scan rate of 2400 nm min^{-1}, using Cary Win UV scan Application software.

2.2. Spectra Collection and Data Treatment. For a solution of multiple absorbing species, the experimental absorption data could be analyzed using the Lambert−Beer law: $A(\lambda) = \sum \varepsilon_i(\lambda) b C_i$, where $A(\lambda)$ and $\varepsilon_i(\lambda)$ (L mol^{-1} cm^{-1}) are the absorbance and molar absorptivity of the absorbing species at wavelength λ, respectively, C_i (mol L^{-1}) is the molar concentration, and b (cm) is the optical path length. However, a different concentration scale, molality (mol/kg of solvent) or specific molality (m_i*; mol/kg of solution), is commonly used in studies under hydrothermal conditions to account for the thermal expansion of the solution as the temperature increases. The expression for the Lambert−Beer law in terms of specific molality is given by

$$A(\lambda)_m = \sum \varepsilon_i(\lambda)\, b m_i^* \quad (2)$$

where $A(\lambda)_m$ (or A_m in the figures) is the corrected absorbance $A(\lambda)_m = A(\lambda)/\rho_{solution}$. Because the solutions are diluted, and for the purpose of this work, the density of the solution, $\rho_{solution}$ (g cm^{-3}), was approximated to that of water at the same temperature and pressure (0.998, 0.961, 0.920, 0.868, and 0.802 at 298, 373, 423, 473, and 523 K, respectively, at 70 bar).[14]

It is worth noting that in the case of HQ, the first few spectra showed two distinct peaks, one at λ_{max} = 244 nm, assigned to BQ, due to partial oxidation of HQ to BQ in the first section of the injection loop, and another at λ_{max} = 289 nm, associated with HQ, in good agreement with other studies.[15] A few minutes after the solution was injected into the cell, only one peak was observed at 289 nm due to HQ. The fact that the absorbance at this wavelength does not change with time is also an indication that water has been displaced, and the concentration of HQ in the cell is equal to that in the original solution.

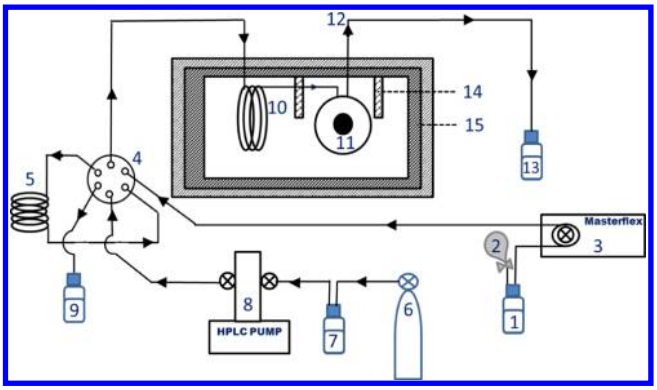

Figure 1. UV−visible flow cell and high-pressure injection system: (1) solution, (2) nitrogen balloon, (3) peristaltic pump, (4) six-port valve, (5) PEEK injection loop, (6) nitrogen gas, (7) deionized water, (8) HPLC pump, (9) waste, (10) titanium preheater, (11) titanium cell, (12) outlet, (13) waste, (14) heater, and (15) ceramic insulation.

2.3. Computer Simulations. Classical MD simulations were performed, using the Amber MD Package,[10] to study the solvation of both HQ and BQ under different conditions of temperature and pressure.

The water model chosen was TIP4P/2005, which has been found to perform well under extreme temperature conditions.[16] The system contained one molecule of quinone (either BQ or HQ) surrounded by 1220 water molecules in a truncated octahedral box. The required HQ and BQ parameters were obtained from Hartree−Fock (HF)-level simulations (in vacuum), using the 6-31G* basis set, and the Restrained Electrostatic Potential method. This RESP approach involves calculating the electrostatic potential of a molecule at HF/6-31G* level of theory, then fitting the classical Coulomb-electrostatic force field to the quantum-level result. With this

DOI: 10.1021/acs.jpcb.6b07893
J. Phys. Chem. B 2016, 120, 10547−10552

electrostatic field, the partial charges of the aforementioned molecule are obtained. In the Amber force field, this is the standard procedure.[17]

The systems were first stabilized at different temperatures and pressures, using a Langevin dynamics thermostat (g_{ln}) and isotropic position scaling. After stabilization, a run of MD (50 ns, time step of 2 fs) was performed. The conditions adopted include 300 K at 1 bar and 300, 373, 423, 473, and 523 K at 70 bar.

In addition, linear response TD-DFT calculations were performed with PCM[11] for describing solvent effects, using Gaussian 09 software.[12] Both the static and optical dielectric constants were adjusted to the proper values at the corresponding temperatures and pressures,[18,19] to simulate the varying conditions. The basis sets used were 6-311+G and aug-cc-pvTZ, whereas three exchange correlation functionals were tested: PBE,[20] B3LYP,[21] and M06-2X.[22] Previous results by Barone et al.[23] showed that the combination of the M06-2X functional with the 6-311+G basis set yielded excellent results for the spectroscopic properties of quinones at room temperature. The conditions adopted include 300, 423, and 473 K, all at the same pressure of 70 bar. The geometries were previously optimized in vacuo using the PBE functional.

3. RESULTS AND DISCUSSION

3.1. Analysis of Spectral Data. Figure 2 shows the UV−visible spectra for BQ and HQ in aqueous 0.2 M $NaHSO_4$, after

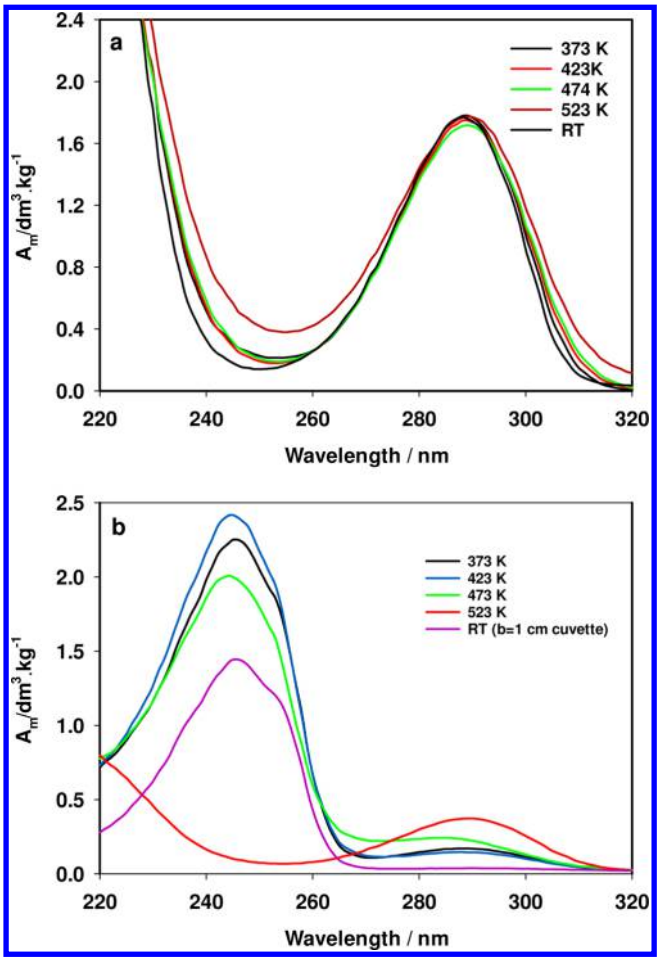

Figure 2. UV−visible corrected spectra for (a) HQ and (b) BQ at 298 K at 1 bar and 373, 423, 473, and 523 K at 70 bar.

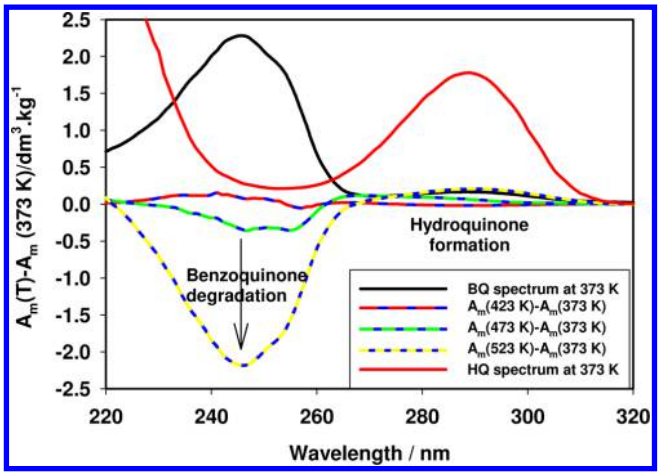

Figure 3. Difference spectra $(A_m(T) - A_m(373\ K))$ for 0.07 mM BQ in 0.2 M Na_2HSO_4 at 423, 473, and 523 K and 70 bar. Reference spectrum: 0.07 mM BQ at 373 K. Spectra were corrected to account for the thermal expansion of the solutions.

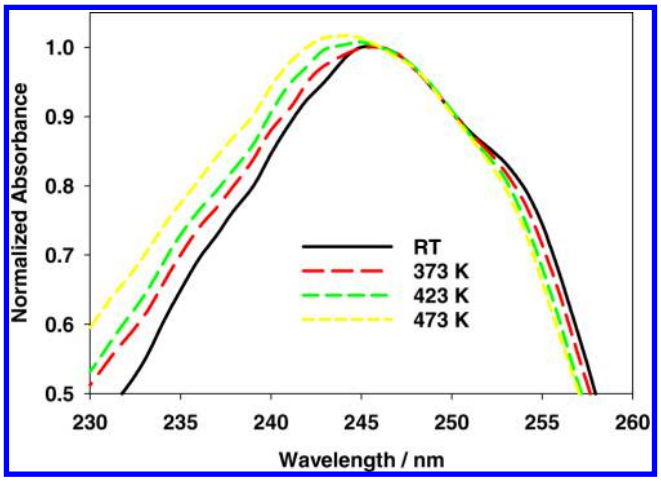

Figure 4. Normalized UV−visible absorption spectra for 0.07 mM BQ in 0.2 M $NaHSO_4$ under ambient conditions and at 373, 423, and 473 K at 70 bar.

Table 1. Effect of Solvent Dielectric Constant on the Wavelength of BQ Absorption Maximum

T (°C)	p (bar)	ε (H_2O)[a]	λ_{max} (nm) (this study)	solvent/ε (solvent)[b]	λ_{max}[b] (nm)
25	1	78.5	246	water	246
100	70	57.7	246		
150	70	46.3	245	glycerol/42.5	246
200	70	37.3	244	acetonitrile/37.5	242
				methanol/32.7	243
250	70	30.0			
				iso-octane/1.94	240

[a]Uematsu and Frank.[24] [b]Ahmed and Khan.[15]

baseline correction using the spectra of a 0.2 M $NaHSO_4$ solution at the same T and p and the density of water to account for changes in the concentration due to thermal expansion. At room temperature, the spectrum of HQ (Figure 2a) shows a main absorption band at 289 nm, and there is a pronounced increase in absorbance at lower wavelengths; the almost negligible change in the spectra is an indication of the thermal stability of HQ under these conditions. At 523 K, the difference in the spectrum of HQ

DOI: 10.1021/acs.jpcb.6b07893
J. Phys. Chem. B 2016, 120, 10547−10552

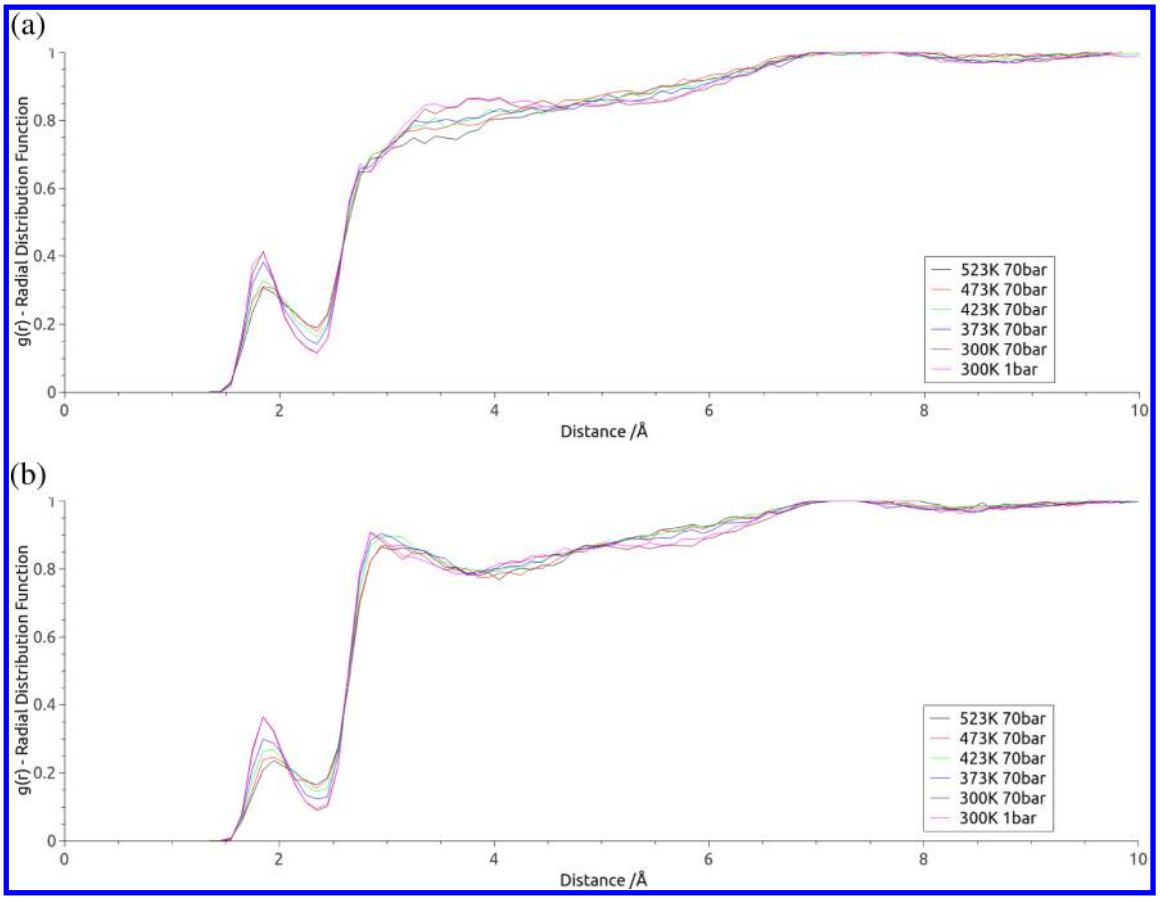

Figure 5. (a) Normalized radial distribution function of water around the O atoms of BQ as a function of temperature. (b) Normalized radial distribution function of water around the O atoms of HQ as a function of temperature.

is attributed to the presence of oxygen, as a leak was observed on experiment completion. The position of the absorption band does not show any significant difference between 298 and 523 K, despite the dielectric constant of water at the highest temperature being significantly smaller, and changes in the positions of the electronic absorption bands can be due to solute−solvent interactions and hydrogen bonding. This is consistent with the TD-DFT calculation results, which predict a very small shift in the absorption bands with temperature in the considered range.

For BQ (Figure 2b), the main absorption band at room temperature is observed at 244 nm, with a shoulder at a higher wavelength. The positions of these bands are in good agreement with those reported for the same ($\pi \rightarrow \pi^*$) transitions in other studies under ambient conditions.[15]

The difference spectra obtained using a low-temperature spectrum as reference was analyzed to better understand the extent of changes in the BQ spectra with temperature (Figure 3). The negative band centered at around 244 nm in Figure 3 indicates that BQ decomposition is almost complete after 15 s at 523 K and 70 bar.

The position of the new band is in excellent agreement with that of HQ in Figure 2a and the calculated spectra (vide infra). This finding is in good agreement with the that from the studies by Razimov et al.[3] and Xu et al.[2] However, the conversion is faster in hot compressed acid media, only a few seconds are required to convert BQ to HQ and other nonabsorbing condensation products at 473 K, and the yield of HQ is also extremely low when compared to that reported by Xu et al.[2], 60% of BQ conversion after 2 h and a 37% HQ yield in SCW.

Despite BQ decomposition, the normalized spectra of BQ instead of the original spectra could be used to investigate the effect of temperature on the position of the main absorption band. As shown in Figure 4, there is a there is a blueshift of the main absorption BQ band as the temperature increases and dielectric constant of water decreases.

Ahmed and Khan[15] reported a similar blueshift while studying the solvent effect (solvent polarity or dielectric constant) on the $\pi \rightarrow \pi^*$ transition energy of benzoquinones at room temperature. An analysis of the solvents used in this study reveals that some of them have a dielectric constant similar to that of water at high T and p, allowing a comparison between studies. The results are summarized in Table 1.

3.2. Simulations. In Figure 5, the radial distributions of H atoms corresponding to water molecules around the oxygen atoms of HQ and BQ are presented as a function of temperature. For BQ, a maximum is found near 1.9 Å, corresponding to water−BQ H-bonds; in a similar manner, maxima are found near 1.9 Å (−OH from HQ acting as a H-acceptor) and 3.9 Å (−OH from HQ acting as a H-donor). These maxima reduce in intensity with increasing temperature, meaning there is an average loss of water coordination around the oxygen atoms of HQ and BQ. A possible cause for the shift in the spectral maxima in BQ is this weakening of H-bonds, mainly by stabilization of the molecule's ground state over the excited state (thus shifting the transition to higher energies). Typical snapshots of solvated BQ and HQ extracted from the MD simulation are shown in Figure 6.

The effect of temperature on the predicted spectra has been modeled by performing TD-DFT calculations using the PCM

DOI: 10.1021/acs.jpcb.6b07893
J. Phys. Chem. B 2016, 120, 10547−10552

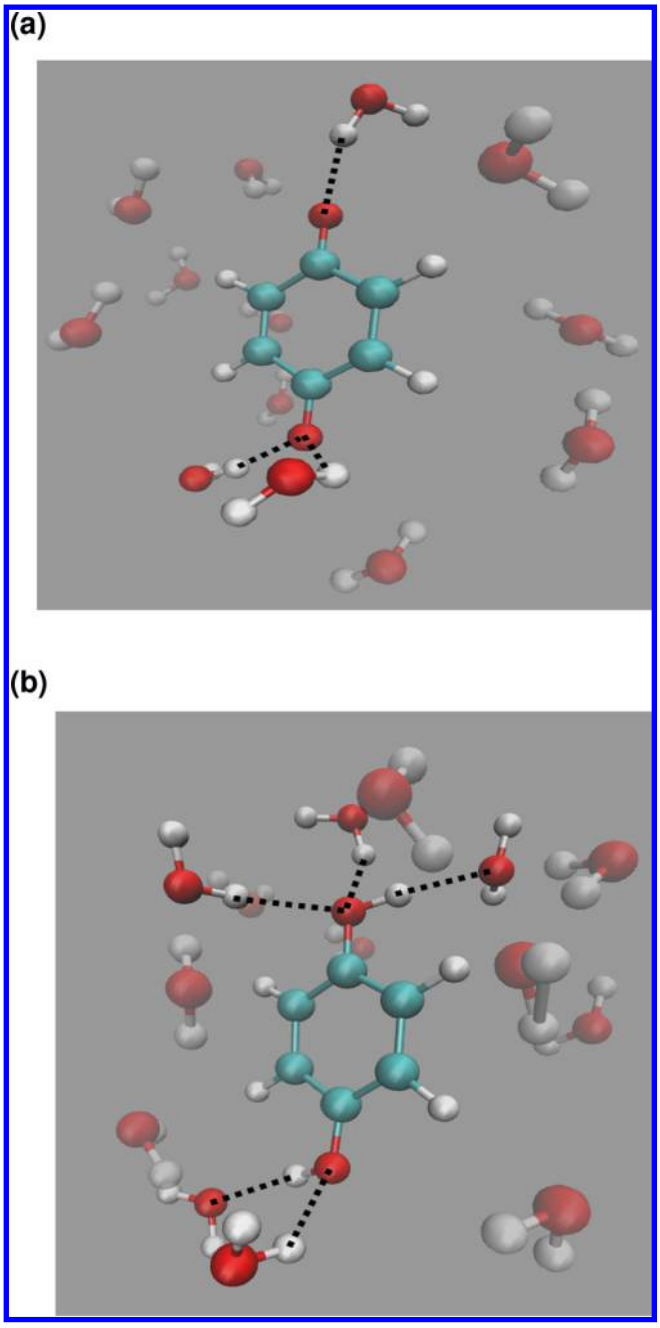

Figure 6. Typical snapshots of the MD simulation depicting the first solvation shell for BQ(a) and HQ(b).

Table 2. Simulations of the Effect of Solvent Dielectric Constant on the Wavelength of BQ Absorption Maximum at 70 bar and Different Temperatures

	λ_{max} (nm)			
	PBE	B3LYP	M06-2X	
T (°C)	6-311+G	6-311+G	6-311+G	aug-cc-pvTZ
25	284.7	267.2	246.8	247.0
150	284.2	266.8	246.3	
200	283.9	266.4	245.9	246.2

[a]Three functionals (PBE, B3LYP, and M06-2X) and two basis sets (6-311+G and aug-cc-pvTZ) were used.

Table 3. Simulations of the Effect of Solvent Dielectric Constant on the Wavelength of HQ Absorption Maximum at 70 bar and Different Temperatures

	λ_{max} (nm)			
	PBE	B3LYP	M06-2X	
T (°C)	6-311+G	6-311+G	6-311+G	aug-cc-pvTZ
25	280.7	260.8	245.7	256.4
150	280.6	260.8	245.6	
200	280.6	260.7	245.6	256.5

[a]The conditions are the same as those used for BQ spectra simulation.

model to describe the changes in the dielectric constant of the solvent. The results of these calculations were consistent with the experiments (Tables 2 and 3). Although the position of the absorption maxima depends heavily on the exchange correlation functional used, a blueshift between 300 and 473 K of about 0.8−0.9 nm is observed for BQ in all cases, whereas for HQ, the shift is around 0.1 nm. The obtained shift for BQ reproduces the same trend as that in the experiment; however, probably because of limitations in the continuum solvent description, the agreement is not quantitative. On the other hand, the result for HQ is consistent with the impossibility to measure such a small shift, thus keeping the maxima in the same position regardless of temperature.

To account for possible specific H-bonding effects, not taken into consideration by the PCM model, we performed additional calculations for BQ (M06-2X functional, 6-311+G basis set) in which water molecules were explicitly included in the calculations. Specifically, we have performed calculations in which the system included one to six water quantum-mechanically treated molecules. Results indicated that the shift involving H-bonds depended mainly on how many waters were coordinated to each oxygen atom of BQ but did not rely on the geometry of such bonds (e.g., changing the angle in which the water was coordinating the oxygen did not affect the position of the absorption maximum predicted by TD-DFT). This allowed us to perform TD-DFT calculations on each configuration accessible by the system, making a weighted average of the obtained spectra. The weights used were obtained from the original classical MD, counting the times each configuration was visited. This resulted in a blueshift of 1.1 nm, which, although a little higher than the shift obtained with BQ alone (0.9 nm), does not reach the experimental value (3 nm).

4. CONCLUSIONS

This study showed the potential of UV−visible spectroscopy as an experimental tool for studying the mechanism of decomposition of benzoquinones under hydrothermal conditions. In good agreement with previous studies, HQ was shown to be stable in acid medium up to 473 K at 70 bar; above this temperature, at 523 K, the decomposition processes can be due to the presence of oxygen, confirming the findings of Bard's group. The reduction of BQ to HQ has also been confirmed from the absorption spectra of BQ as a function of temperature. The conversion is not quantitative, but the formation of other absorbing hydroxylated quinones was not observed between 373 and 523 K at 70 bar.

The classical simulation approach with explicit water at different temperatures allows us to see how the structure of solvation changes with temperature. On the other hand, electronic spectra calculations performed on the basis of TD-

DOI: 10.1021/acs.jpcb.6b07893
J. Phys. Chem. B 2016, 120, 10547−10552

DFT showed good agreement with the experimental results, obtaining a blueshift of 0.9 nm for BQ (and a smaller blueshift of 0.1 nm for HQ) when changing the temperature from 300 to 423 K. The shift was mainly related to the change in the dielectric constant of the solvent, which agrees with the results obtained using different solvents.

AUTHOR INFORMATION

Corresponding Authors

*E-mail: dario.estrin@gmail.com. Tel: 5411-4576-3378/79/80 ext. 105 (D.A.E.).

*E-mail: liliana.trevani@uoit.ca. Tel: 905-721-8668 ext. 3430 (L.T.).

Author Contributions

§F.S. performed the experiments, whereas F.N.P. was responsible for the computational calculations; both students made significant contributions to this work.

Notes

The authors declare no competing financial interest.

ACKNOWLEDGMENTS

This work was supported by the Natural Sciences and Engineering Research Council of Canada through the Discovery Grants Program section, the Faculty of Science at the University of Ontario Institute of Technology, and the University of Buenos Aires, UBACYT.

REFERENCES

(1) Liu, C. Y.; Snyder, S. R.; Bard, A. J. Electrochemistry in Near-Critical and Supercritical Fluids. 9. Improved Apparatus for Water Systems (23−385 °C). The Oxidation of Hydroquinone and Iodide. *J. Phys. Chem. B* **1997**, *101*, 1180−1185.

(2) Xu, T.; Liu, Q.; Liu, Z.; Wu, J. The Role of Supercritical Water in Pyrolysis of Carbonaceous Compounds. *Energy Fuels* **2013**, *27*, 3148−3153.

(3) Razimov, A. V.; Bekmashi, F. T.; Liogon'kii, B. I. Thermal Polymerization of p-Benzoquinone. *Polym. Sci. U.S.S.R.* **1975**, *17*, 3164−3170.

(4) Kaurola, P.; Sharma, V.; Vonk, A.; Vattulainen, I.; Róg, T. Distribution and Dynamics of Quinones in the Lipid Bilayer Mimicking the Inner Membrane of Mitochondria. *Biochim. Biophys. Acta, Biomembr.* **2016**, *1858*, 2116−2122.

(5) Ensafi, A. A.; Jamei, H. R.; Heydari-Bafrooei, E.; Rezaei, B. Electrochemical Study of Quinone Redox Cycling: A Novel Application of DNA-Based Biosensors for Monitoring Biochemical Reactions. *Bioelectrochemistry* **2016**, *111*, 15−22.

(6) Nueangnoraj, K.; Tomai, T.; Nishihara, H.; Kyotani, T.; Honma, I. An Organic Proton Battery Employing Two Redox-Active Quinones Trapped within the Nanochannels of Zeolite-Templated Carbon. *Carbon* **2016**, *107*, 831−836.

(7) Ishii, Y.; Tashiro, K.; Hosoe, K.; Al-zubaidi, A.; Kawasaki, S. Electrochemical Lithium-Ion Storage Properties of Quinone Molecules Encapsulated in Single-Walled Carbon Nanotubes. *Phys. Chem. Chem. Phys.* **2016**, *18*, 10411−10418.

(8) Lin, K.; Chen, Q.; Gerhardt, M. R.; Tong, L.; Kim, S. B.; Eisenach, L.; Valle, A. W.; Hardee, D.; Gordon, R. G.; Aziz, M. J.; Marshak, M. P. Alkaline Quinone Flow Battery. *Science* **2015**, *349*, 1529−1532.

(9) Tossell, J. A. Quinone−Hydroquinone Complexes as Model Components of Humic Acids: Theoretical Studies of their Structure, Stability and Visible−UV Spectra. *Geochim. Cosmochim. Acta* **2009**, *73*, 2023−2033.

(10) Pearlman, D. A.; Case, D. A.; Caldwell, J. W.; Ross, W. S.; Cheatham, T. E.; DeBolt, S.; Ferguson, D.; Seibel, G.; Kollman, P. AMBER, a Package of Computer Programs for Applying Molecular Mechanics, Normal Mode Analysis, Molecular Dynamics and Free Energy Calculations to Simulate the Structural and Energetic Properties of Molecules. *Comput. Phys. Commun.* **1995**, *91*, 1−41.

(11) Scalmani, G.; Frisch, M. J. Continuous Surface Charge Polarizable Continuum Models of Solvation. I. General Formalism. *J. Chem. Phys.* **2010**, *132*, No. 114110.

(12) Frisch, M. J.; Trucks, G. W.; Schlegel, H. B.; Scuseria, G. E.; Robb, M. A.; Cheeseman, J. R.; Scalmani, G.; Barone, V.; Mennucci, B.; Petersson, G. A.; Nakatsuji, H.; Caricato, M.; Li, X.; Hratchian, H. P.; Izmaylov, A. F.; Bloino, J.; Zheng, G.; Sonnenberg, J. L.; Hada, M.; Ehara, M.; Toyota, K.; Fukuda, R.; Hasegawa, J.; Ishida, M.; Nakajima, T.; Honda, Y.; Kitao, O.; Nakai, H.; Vreven, T.; Montgomery, J. A., Jr.; Peralta, J. E.; Ogliaro, F.; Bearpark, M. J.; Heyd, J.; Brothers, E. N.; Kudin, K. N.; Staroverov, V. N.; Kobayashi, R.; Normand, J.; Raghavachari, K.; Rendell, A. P.; Burant, J. C.; Iyengar, S. S.; Tomasi, J.; Cossi, M.; Rega, N.; Millam, N. J.; Klene, M.; Knox, J. E.; Cross, J. B.; Bakken, V.; Adamo, C.; Jaramillo, J.; Gomperts, R.; Stratmann, R. E.; Yazyev, O.; Austin, A. J.; Cammi, R.; Pomelli, C.; Ochterski, J. W.; Martin, R. L.; Morokuma, K.; Zakrzewski, V. G.; Voth, G. A.; Salvador, P.; Dannenberg, J. J.; Dapprich, S.; Daniels, A. D.; Farkas, Ö.; Foresman, J. B.; Ortiz, J. V.; Cioslowski, J.; Fox, D. J. *Gaussian 09*; Gaussian, Inc.: Wallingford, CT, 2009.

(13) Trevani, L. N.; Roberts, J. C.; Tremaine, P. R. Copper(II)-Ammonia Complexation Equilibria in Aqueous Solutions at Temperatures from 30 to 250 °C by Visible Spectroscopy. *J. Solution Chem.* **2001**, *30*, 585−622.

(14) Lemmon, E. W.; Huber, M. L.; McLinden, M. O. *NIST Standard Reference Database 23: Reference Fluid Thermodynamic and Transport Properties-REFPROP*, version 9.1; National Institute of Standards and Technology, Standard Reference Data Program: Gaithersburg, MD, 2013.

(15) Ahmed, M.; Khan, Z. H. Electronic Absorption Spectra of Benzoquinone and its Hydroxy Substituents and Effect of Solvents on their Spectra. *Spectrochim. Acta, Part A* **2000**, *56*, 965−981.

(16) Abascal, J. L. F.; Vega, C. A General Purpose Model for the Condensed Phases of Water: TIP4P/2005. *J. Chem. Phys.* **2005**, *123*, No. 234505.

(17) Bayly, C. I.; Cieplak, P.; Cornell, W.; Kollman, P. A. A Well Behaved Electrostatic Potential Based Method Using Charge Restraints for Deriving Atomic Charges: The RESP Model. *J. Phys. Chem.* **1993**, *97*, 10269−10280.

(18) Kaatze, U. Complex Permittivity of Water as a Function of Frequency and Temperature. *J. Chem. Eng. Data* **1989**, *34*, 371−374.

(19) Putintsev, N. M.; Putintsev, D. N. High-Frequency Dielectric Permittivity of Water and its Components. *Russ. J. Phys. Chem. A* **2011**, *85*, 1113−1118.

(20) Perdew, J. P.; Burke, K.; Ernzerhof, M. Generalized Gradient Approximation Made Simple. *Phys. Rev. Lett.* **1996**, *77*, 3865−3868.

(21) Becke, A. D. A New Mixing of Hartree−Fock and Local Density-Functional Theories. *J. Chem. Phys.* **1993**, *98*, 1372−1377.

(22) Zhao, Y.; Truhlar, D. G. The M06 Suite of Density Functionals for Main Group Thermochemistry, Thermochemical Kinetics, Noncovalent Interactions, Excited States, and Transition Elements: Two New Functionals and Systematic Testing of Four M06-Class Functionals and 12 Other Functionals. *Theor. Chem. Acc.* **2008**, *120*, 215−241.

(23) Barone, V.; Cacelli, I.; Crescenzi, O.; d'Ischia, M.; Ferretti, A.; Prampolini, G.; Villani, G. Unraveling the Interplay of Different Contributions to the Stability of the Quinhydrone Dimer. *RSC Adv.* **2014**, *4*, 876−885.

(24) Uematsu, M.; Frank, E. U. Static Dielectric Constant of Water and Steam. *J. Phys. Chem. Ref. Data* **1980**, *9*, 1291−1306.

DOI: 10.1021/acs.jpcb.6b07893
J. Phys. Chem. B 2016, 120, 10547−10552